

# Impact Testing and Analysis for Structural Code Benchmarking\*

R.E. Glass

*Sandia National Laboratories\*\*, Albuquerque, New Mexico, United States of America*

## INTRODUCTION

Sandia National Laboratories, in cooperation with industry and other national laboratories, has been benchmarking computer codes ("Structural Code Benchmarking for the Analysis of Impact Response of Nuclear Material Shipping Casks," R. E. Glass, Sandia National Laboratories, 1985; "Sample Problem Manual for Benchmarking of Cask Analysis Codes," R. E. Glass, Sandia National Laboratories, 1988; "Standard Thermal Problem Set for the Evaluation of Heat Transfer Codes Used in the Assessment of Transportation Packages, R. E. Glass, et al., Sandia National Laboratories, 1988) used to predict the structural, thermal, criticality, and shielding behavior of radioactive materials packages. The first step in the benchmarking of the codes was to develop standard problem sets and to compare the results from several codes and users. This step for structural analysis codes has been completed as described in "Structural Code Benchmarking for the Analysis of Impact Response of Nuclear Material Shipping Casks," R. E. Glass, Sandia National Laboratories, 1985. The problem set is shown in Fig. 1. This problem set exercised the ability of the codes to predict the response to end (axisymmetric) and side (plane strain) impacts with both elastic and elastic/plastic materials.

The results from these problems showed that there is good agreement in predicting elastic response. Significant differences occurred in predicting strains for the elastic/plastic models. An example of the variation in predicting plastic behavior is given in Fig. 2, which shows the hoop strain as a function of time at the impacting end of Model B. These differences in predicting plastic strains demonstrated a need for benchmark data for a cask-like problem.

## TEST DESCRIPTION

The primary objective in defining the tests used to obtain benchmark data was to simulate the elastic/plastic response encountered in actual package containment boundaries subjected to the regulatory 30-foot free drop. This requirement was met by designing a thick-walled cylinder and by performing a guided drop equivalent to a 30-foot drop onto an unyielding target. The test articles were constructed of 6061-T6 aluminum to provide significant plastic deformation and, hence, provide an upper bound on the deformation that would be seen in more typical steel cask structures. In addition, aluminum material properties are relatively strain rate independent ( $\pm 10$  percent) at the test strain rates. The response was made more severe by dropping the test article on the target without an impact limiter.

A secondary objective was to make the test article simple to analyze. This objective was met with a cylindrical design undergoing a flat ( $\pm 1^\circ$ ) end impact. This test can be analyzed with a simple 2-D axisymmetric model. The test geometry is given in Fig. 3, and the material properties based on four samples are given in Table I.

\*This work performed at Sandia National Laboratories, Albuquerque, New Mexico, supported by the U. S. Department of Energy under Contract DE-AC04-76DP00789. \*\*A United States Department of Energy Facility

Table I: Measured Properties for 6061-T0 Aluminum Test Article

	Young's Modulus (psi)	Yield Stress (psi)	Hardening Modulus (psi)
Mean	$12.20 \times 10^6$	9196	$2.87 \times 10^5$
Standard Deviation	$0.32 \times 10^6$	326	$0.64 \times 10^5$

The instrumentation for the tests is also shown in Fig. 3. It consists of eight strain rosettes located at 1 and 3 inches from the impacting end at  $0^\circ$ ,  $90^\circ$ ,  $180^\circ$ , and  $270^\circ$  around the perimeter. These strain gages were used to determine the axial and hoop strains. In addition to the strain gages, two accelerometers were mounted at the top of the test articles. The data from the accelerometers, which was filtered with a Butterworth filter with a cutoff frequency of 1,000 Hz, provided the rigid body deceleration. During the tests, high-speed photography (2,000 fps) was used to obtain impact and rebound velocities and to confirm that the angle of impact was less than  $1^\circ$  from perpendicular. The test articles were inspected pre- and post-test to determine total deformations.

## TEST RESULTS

The complete data from the four tests are presented in "Structural Code Benchmarking Data Report," R. E. Glass, Sandia National Laboratories, to be released. The data consists of the photometrics results, the strain histories, and the accelerometer data filtered at 10,000 Hz (wideband) and 1,000 Hz. The data were filtered at 1,000 Hz to eliminate the vibrational modes and, hence, yield the rigid body response.

The results from Benchmark E are reviewed to serve as an example of all benchmark tests. Examples of the accelerometer data from Benchmark E are given in Figs. 4 and 5. Fig. 4 shows the acceleration data filtered at 10,000 Hz. This data includes the rigid body response as well as the vibrational modes. These vibrational modes are most apparent in the damped first fundamental mode of 2,200 Hz. Each accelerometer channel shows the same signal indicating a flat impact. This was verified by analysis of the photometric data showing a  $0.8^\circ$  offset at impact. Previous work described in "Testing the Half-Scale Model of the Defense High-Level Waste Transportation Cask," M. M. Madsen, et al., Sandia National Laboratories, 1987, indicates that these data are accurate to  $\pm 15$  percent. Fig. 5 shows the Benchmark E data filtered at 1,000 Hz. This data is representative of the rigid body deceleration. The peak rigid body deceleration from Fig. 5 is 2,700 g.

Strain gage data provided the axial and hoop strains at 1 and 3 inches from the impacting end and at the  $0^\circ$ ,  $90^\circ$ ,  $180^\circ$ , and  $270^\circ$  locations around the perimeter. From the timing of the signals, the angle of the test article caused it to impact first between locations 2 and 3. The time delay of 0.07 milliseconds between the strain at locations 2 and 3 and strains at locations 1 and 4 corresponds to a travel of 0.037 inch at the 527 inches per second impact velocity. This corresponds to an impact angle of  $0.4^\circ$ , again verifying an impact within the  $1^\circ$  bound. The data show the strains peaking at from 4,000 to 6,000 microstrain followed by an elastic rebound with a permanent strain resulting from plastic deformation. The permanent strains range from 3,500 to 5,400 microstrain.

The axial strains provide greater deformations. The negative strains indicate compression. The average peak and permanent strains over the four benchmark tests are given in Table II.

The rebound velocities are obtained from the photometric data. The known diameter of the test article is used as the reference length for obtaining frame-to-frame displacements, and the timing signal on the film is used to measure elapsed time. Similarly, the change in displacement from frame to frame is used to obtain velocity. Since the rate of change of velocity is constant, the velocity at impact and rebound are obtained with straight line extrapolations to time 0. The average rebound velocity was 9.5 ft/sec with a standard deviation of 0.3 ft/sec.

Permanent deformations were obtained from the pre- and post-test inspection of the test articles. The total axial deformations are given in Table II.

## ANALYSIS RESULTS

A standard problem has been defined based on the test geometry and materials. The problem is an axisymmetric two-dimensional problem. The results for an off-axis impact are also presented. The analyses were performed using the PRONTO-2D and PRONTO-3D codes as described in "PRONTO-2D: A Two-Dimensional Transient Solid Dynamics Program," L. M. Taylor and D. P. Flanagan,

Sandia National Laboratories, 1987. The geometry is given in Fig. 3. The material properties, derived from the average of the measured data, are given in Table I.

The target was treated as a flat horizontal rigid surface. The friction coefficient between the target and the test article was selected to match the experimental radial displacement of the test article at the target/test article interface. This friction coefficient is 0.05.

A second problem was run using PRONTO-3D with an off-axis impact angle of 0.2°. The material properties are the same as for the first problem. The results for the analyses and the mean and standard deviation values for the four tests are included in Table II. Defining the 0° angle at the impact point, the strains are given at the 0° and 180° locations.

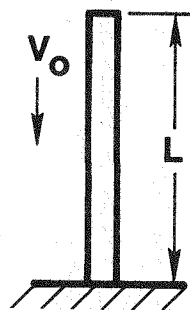
Table II Comparison of Analytical and Experimental Results

	Experiment		Analytical	
	Mean	Standard Deviation	2-D	3-D
Rebound velocity (ft/s)	9.5	0.3	10.9	9.4
Rigid body deceleration (g)	3000	400	2700	2700
Total axial deformation (in)	.170	.022	.137	.135 to .156
Permanent hoop strain (microstrain)				
1 inch	4900	930	4975	4044 to 5700
3 inches	4800	1320	5540	4690 to 5760
Permanent axial strain				
1 inch	-11500	1510	-11,700	-9470 to -13680
3 inches	-12600	2640	-11,600	-9500 to -11820

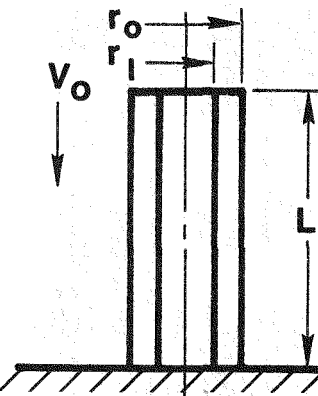
In all cases, the 3-D model falls within one standard deviation of the experimental data. For the 2-D model the rebound velocity is higher, and the total axial deformation is lower. This is an indication of the effect of the off-axis impacts which have a smaller initial area of impact and, hence, greater plastic deformation and lower elastic response.

## CONCLUSION

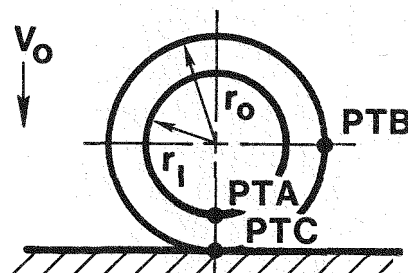
A series of four tests were performed to obtain benchmark data on the structural response of thick-walled structures when subjected to the regulatory 30-foot drop. These data were used to produce the experimentally based benchmark problem that was defined and analyzed in the text. This problem can be used to validate codes which are used to predict the elastic and inelastic response of nuclear materials transportation packages.



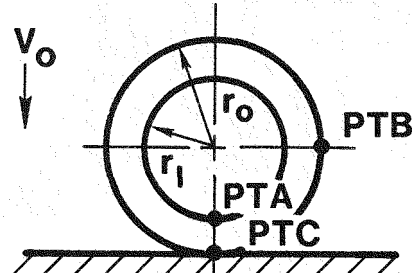
**MODEL A - ELASTIC END IMPACT**



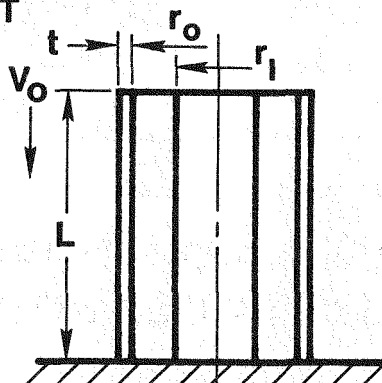
**MODEL B - ELASTIC/PERFECTLY PLASTIC END IMPACT**



**MODEL C - ELASTIC SIDE IMPACT**



**MODEL D - ELASTIC /PERFECTLY PLASTIC SIDE IMPACT**



**MODEL E - ELASTIC/PERFECTLY PLASTIC END IMPACT WITH SLIDING INTERFACES**

Figure 1. Structural Problem Set

Figure 2. Analytical Predictions of Hoop Strain as a Function of Time

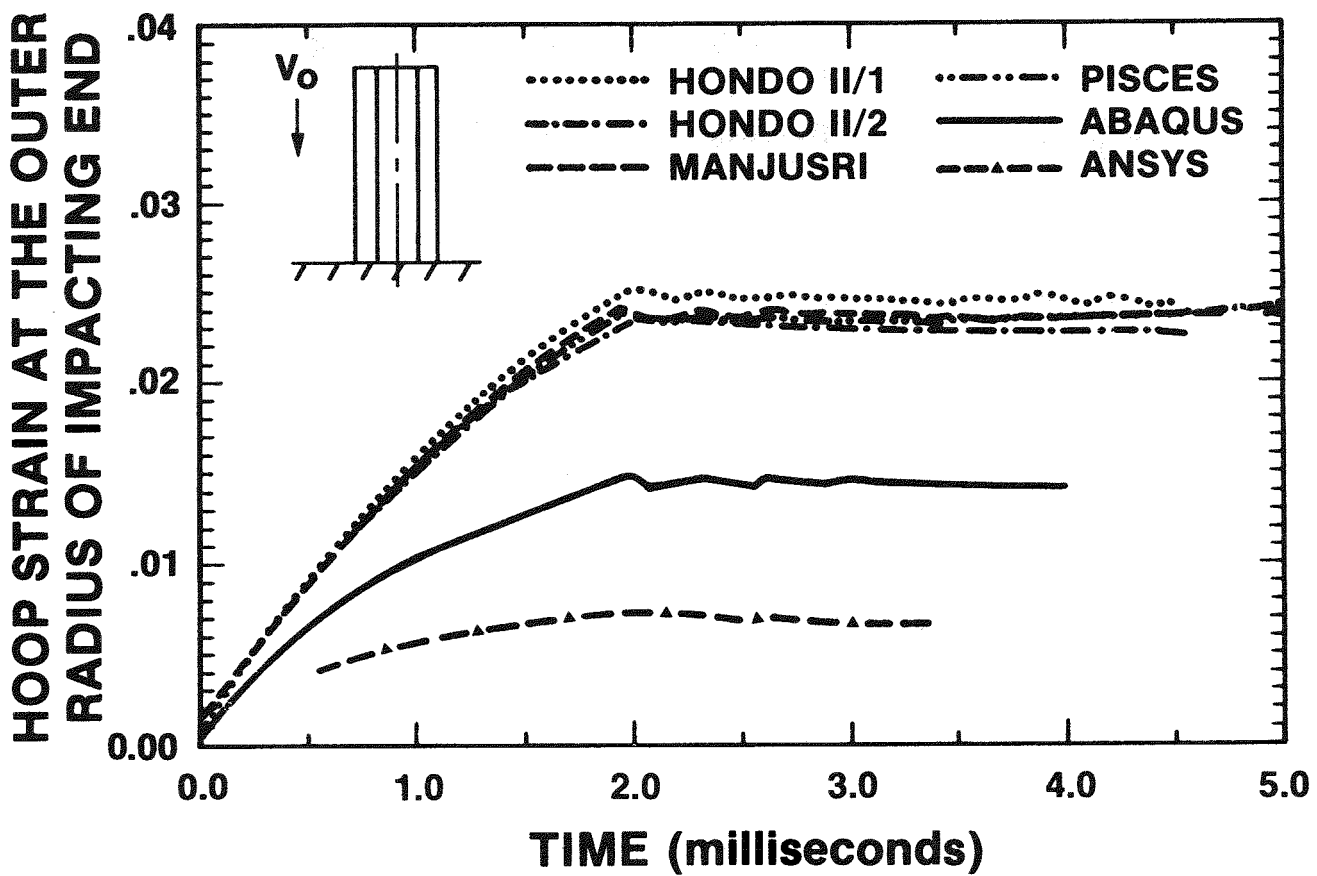
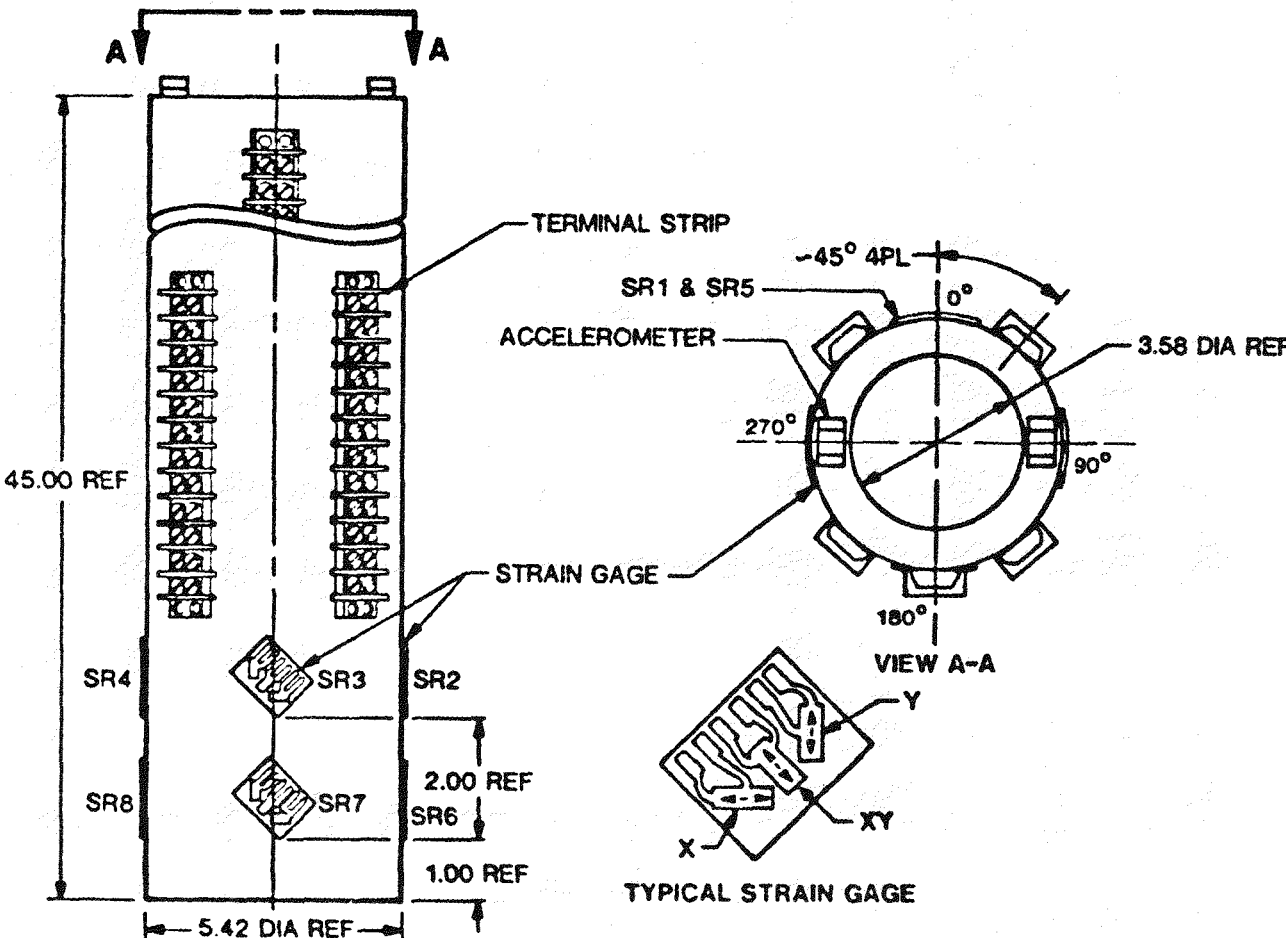


Figure 3. Test Geometry and Instrumentation



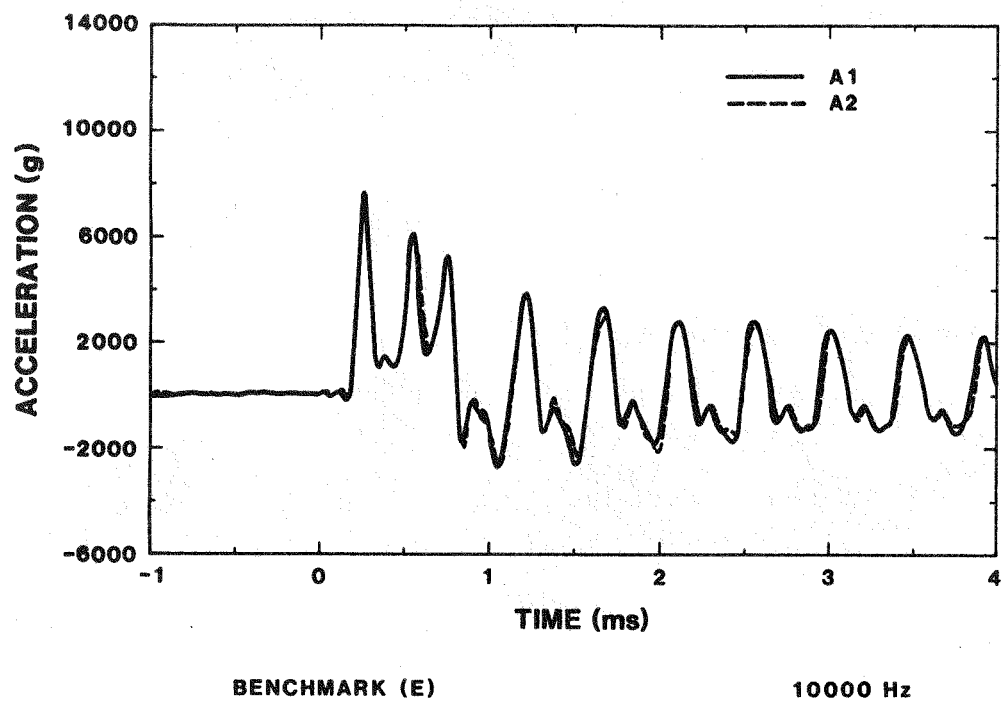


Figure 4. Benchmark E Accelerometer Data--10,000 Hz

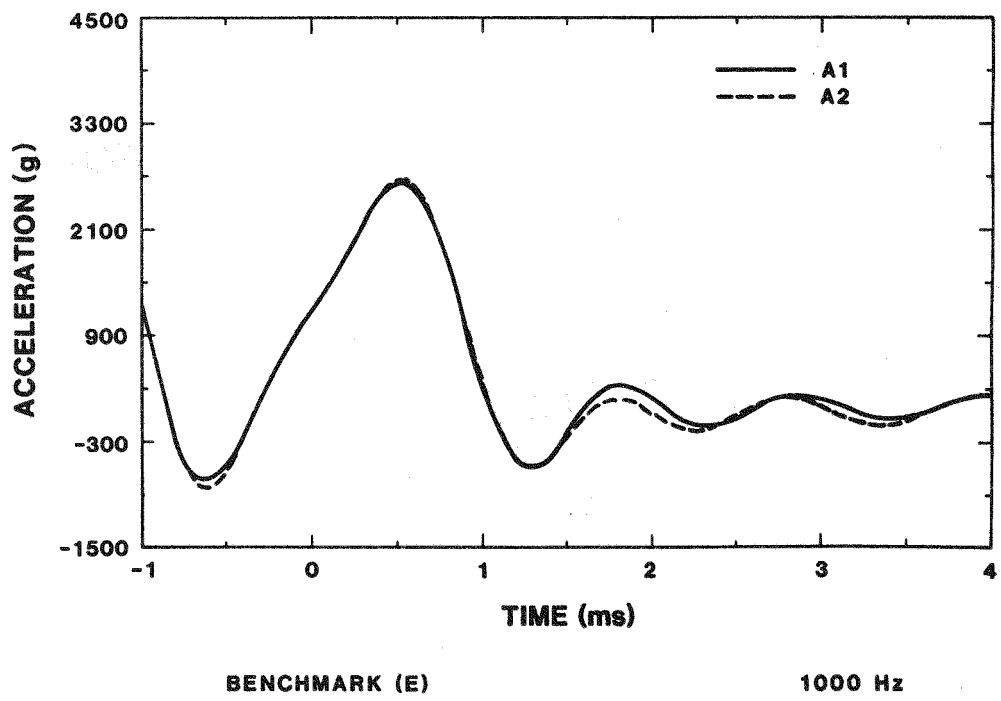


Figure 5. Benchmark E Accelerometer Data--1,000 Hz

## REFERENCES

Glass, R. E. "Structural Code Benchmarking for the Analysis of Impact Response of Nuclear Material Shipping Casks," SAND84-1855C, Sandia National Laboratories, Albuquerque, NM 87185 (1985).

Glass, R. E. "Sample Problem Manual for Benchmarking of Cask Analysis Codes," SAND88-0190, Sandia National Laboratories, Albuquerque, NM 87185 (1988).

Glass, R. E., et al. "Standard Thermal Problem Set for the Evaluation of Heat Transfer Codes Used in the Assessment of Transportation Packages," SAND88-0380, Sandia National Laboratories, Albuquerque, NM 87185 (1988).

Glass, R. E. "Structural Code Benchmarking Data Report," SAND88-3362, Sandia National Laboratories, Albuquerque, NM 87185, to be released.

Madsen, M. M., et al. "Testing the Half-Scale Model of the Defense High-Level Waste Transportation Cask," SAND86-1130, Sandia National Laboratories, Albuquerque, NM 87185, (1987).

Taylor, L. M., and Flanagan, D. P. "PRONTO-2D: A Two-Dimensional Transient Solid Dynamics Program," SAND86-0594, Sandia National Laboratories, Albuquerque, NM 87185, (1987).